TEM Fracture Studies of Polymer Interfaces

Junichiro Washiyama,† Costantino Creton,‡ and Edward J. Kramer*

Department of Materials Science and Engineering, Cornell University, Ithaca, New York 14853

Received March 16, 1992; Revised Manuscript Received April 16, 1992

ABSTRACT: A new transmission electron microscopic technique is described with which it is possible to observe and make quantitative measurements of deformation and fracture mechanisms at planar interfaces between two immiscible homopolymers. Utilizing this technique, we have studied the fracture of interfaces between polystyrene (PS) and poly(2-vinylpyridine) (PVP) homopolymers reinforced with a series of PS–PVP block copolymers. Typically a craze was observed ahead of the crack tip. The craze was formed on the PS side of the interface, as expected, since the crazing stress of PS is lower than that of PVP. Craze breakdown occurred exclusively at the PVP/PS craze interface, showing that the block copolymer reinforced interface was still the weakest link in the material. It was also found that the values of the critical energy release rate of the crack (G_c) calculated from TEM micrographs are comparable to those obtained from conventional fracture toughness tests over a wide range of G_c, indicating that crazing is the dominant energy dissipation mechanism in this system and governs the fracture toughness of the interface.

Introduction

Strong interfacial adhesion and a controlled morphology are particularly important issues for phase-separated blends of immiscible homopolymers. It has been known for some time that additions of block copolymers to these blends cause remarkable improvement in their mechanical properties,[1,2] particularly in their fracture toughness characteristics, and, accordingly, block copolymers have been widely used as compatibilizers for these polymer blend systems. The improvement undoubtedly results from the following two features: First, block copolymer chains segregate to interfaces between the two phases, resulting in a reduction of the interfacial tension (interfacial energy)[3,4] and thereby enabling the formation of smaller scale domains via melt processing.[1,2] Second, block copolymer chains form interphase junctions through which stress can be transferred,[5–8] resulting in a substantial reinforcement of the interfaces themselves.[1,2,5–8] We focus on this second feature in the present study.

Recently experiments[5–8] have examined the reinforcement effects of various combinations of block copolymers added to the interfaces between immiscible homopolymers and observed a remarkable improvement in the fracture toughness, G_c, of the interfaces as a function of molecular weight of both blocks and areal density of the block copolymers. Concurrently, a theoretical model[9–11] has been developed to explain the reinforcement effect of block copolymers at the interfaces between immiscible homopolymers. Creton et al.[7] demonstrated the existence of a critical molecular weight for block copolymer reinforcement of PS/PVP interfaces using quantitative TEM analysis, where they separated the effects on the mechanical strength of the interface from those coming from the phase size and concluded that at least one entanglement between each block and its respective homopolymer was necessary to achieve effective interfacial reinforcement.

Despite many studies on this subject, there have been no direct high-resolution observations to demonstrate which deformation mechanisms are active during fracture of planar interfaces: for instance, crazing, shear deformation, and cavitation could all contribute, in principle, in a given system. Only the optical interference microscopic study of Creton et al.[8] was able to observe a craze at the PS/PVP interface reinforced with PS–PVP block copolymers. The resolution of this technique was on the order of wavelength of light (~550 nm) and was not sufficient to reveal structures on a smaller scale. Similarly, there is no precise knowledge of where the locus of the fracture plane is relative to the interface, although secondary ion mass spectrometry (SIMS)[6] and forward recoil spectrometry (FRES)[6,8] measurements of the location of deuterium-labeled blocks of the block copolymer have allowed important inferences to be drawn. A higher resolution microscopic observation of the deformation and fracture mechanisms at the interface would therefore be useful in order to understand the fracture processes in more detail. The object of this study is to develop an experimental method that will allow quantitative observation of interfacial fracture processes, the observation that will enable conclusions about the fracture mechanisms to be drawn.

We have chosen polystyrene (PS) and poly(2-vinylpyridine) (PVP) homopolymers as an immiscible polymer pair and a PS–PVP block copolymer as a compatibilizer to reinforce the interface between PS and PVP. One of the advantages of this system is that both homopolymers have about the same glass transition temperature and mechanical properties; namely, both of them preferentially deform plastically by crazing,[7,8] which can be easily recognized with transmission electron microscopy (TEM). Furthermore, thermodynamic characteristics, such as the Flory interaction parameter, χ, between PS and PVP are known from previous studies,[12–15] giving us an additional advantage in the understanding this system.

Experimental Section

(1) Materials. PS and PVP homopolymers purchased from Aldrich Chemical Co. Inc. were of commercial grade with weight-average molecular weights of 250 000 and 200 000, respectively. The block copolymers listed in Table I were synthesized by anionic polymerization in tetrahydrofuran (THF) using cumylpotassium as the initiator at −55 °C in an argon atmosphere; all these block copolymers had polydispersity indices of 1.1 or less. The molecular weight and the composition of these block copolymers were characterized using gel permeation chromatography (GPC), forward recoil spectroscopy (FRES),[16,17] and nuclear magnetic resonance (NMR). More details of the polymerization and the characterization can be found elsewhere.[18]

† Visiting scientist from Kawasaki Plastics Laboratory, Showa Denko K.K., 3-2, Chidori-cho, Kawasaki-ku, Kawasaki, Kanagawa, 210, Japan.

‡ Present address: IBM Almaden Research Center, 650 Harry Rd., San Jose, CA 95120.

0024-9297/92/2225-4751$03.00/0

Table I
Polymerization Indices of the Block Copolymers

code	d-PS block	PVP block
A	960[a]	950
B	800	870
C	510	540
D	680	100

[a] The PS block is protonated PS.

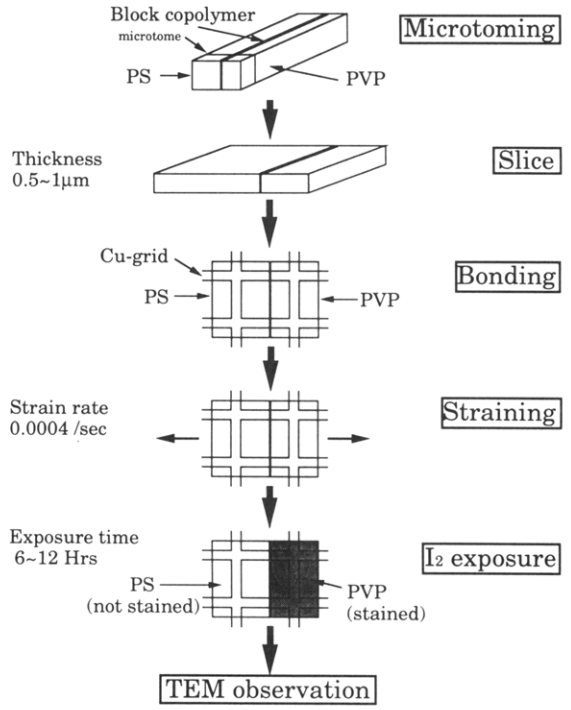

Figure 1. Block diagram of the sample preparation and testing procedure.

The block copolymer consisting of a PS block whose polymerization index is 960 and a PVP block whose polymerization index is 950 will be designated as 960/950. For the block copolymers of A (960/950), B (800/870), and C (510/540), the polymerization indices of both blocks are much larger than the polymerization index between entanglements, N_e, of their respective homopolymers (173 and 255 for PS and PVP, respectively[8]), ensuring that both PS and PVP blocks of these can form entanglements with their respective homopolymer. For the case of block copolymer D (680/100), however, the PVP block cannot form entanglements with PVP homopolymer, since the polymerization index of the PVP block is much smaller than $N_{e,PVP}$.

(2) Sample Preparation. Slabs of PS and PVP were fabricated by compression molding at 160 °C. A thin film of the block copolymer was spun cast from toluene solutions on the PVP slab. The slab was dried at 80 °C, which is well below the T_g of PVP (108 °C), for 2 h in vacuum. This drying process does not induce the diffusion of block copolymer chains into PVP homopolymer. The areal density of block copolymer chains at the interface, Σ, was controlled by varying the concentration of the block copolymer in solution (0.06–2.0%), which determined in turn the thickness of the block copolymer layer; the Σ was measured with FRES. The resulting PVP slab was then joined to the PS slab, annealed in a mold at 160 °C for 2 h, and then allowed to cool to room temperature. In this annealing process, some block copolymer chains diffuse away from the interface while the majority approaches an equilibrium conformation at the interface, i.e., forms junctions between these two phases. The resulting sandwich was then cut with a diamond saw to obtain strips for the fracture toughness measurement.[8] The dimensions of the strips were 50.8 mm long × 8.7 mm wide × 4.0 mm thick (2.3 and 1.7 mm for PS and PVP, respectively). One of these strips was then cut into smaller pieces for the microtomy described in the next section.

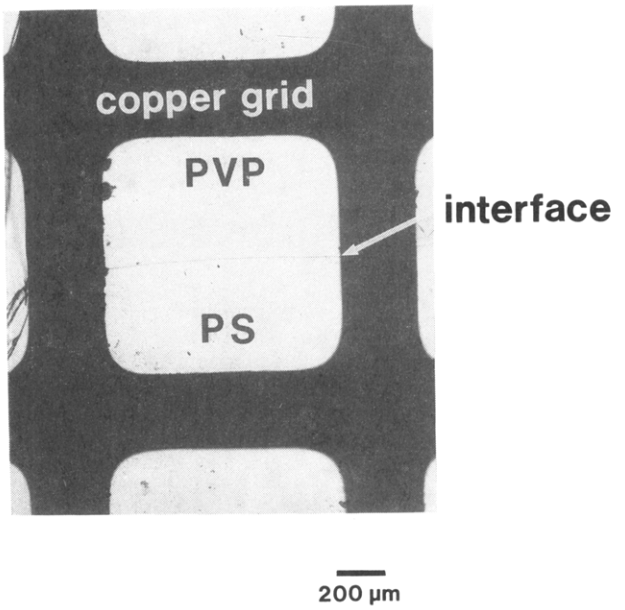

Figure 2. Optical micrograph of a thin film containing an interface bonded to a copper grid.

(3) TEM Observation. We have combined a microtoming method[19] to produce thin films containing the interface and a copper grid technique[20] to strain the microtomed films to allow the observation of the fracture mechanisms at the interfaces by TEM. The block diagram of the procedure is shown in Figure 1. A small piece of the strip was embedded in epoxy resin and cured at room temperature for 2 h and then microtomed with a glass knife at room temperature in a direction perpendicular to the interfacial plane to obtain thin (0.5–1.0-μm) films. The knife angle and the clearance angle were 45° and 9°, respectively. Wrinkles in the film caused by microtoming were removed by briefly exposing the film to solvent (toluene/chloroform = 50/50) vapor. The resulting film was then placed on a ductile copper grid (1 mm × 1 mm grid squares), the grid bars of which had been previously coated with the block copolymer A. It should be noted that the interface must be carefully aligned perpendicular to the straining direction, and hence parallel to grid bars (see Figure 2), so that one can minimize the introduction of the K_{II} fracture mode (in-plane shear) to the interfacial fracture. The grid was then exposed to the vapor of the same solvent mixture for several seconds to ensure good bonding between the grid bars and the film and then dried at 50 °C for 12 h in vacuum to evaporate the solvents and to relax the residual stress.

The resulting grid was strained in tension at a constant strain rate of $\sim 4 \times 10^{-4}$/s with a servo-controlled motor drive at room temperature in air. The plastic deformation of the copper grid ensures that the strain in the polymer film was retained during the TEM observation. The film was then exposed to iodine vapor at room temperature for 6–12 h to stain the PVP phase in the film for the TEM observation. PVP forms a complex with iodine[21] as depicted in eq 1, while PS does not, resulting in enhanced

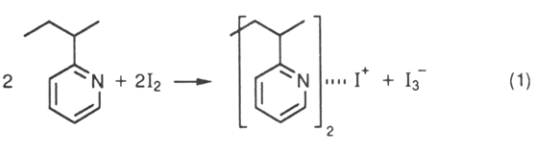

(1)

electron scattering from, and a "darkening" of, the PVP phase which can then be easily distinguished from the less scattering "brighter" phase of PS. This long exposure, however, relaxes craze fibrils, resulting in a coalesced fibril structure of a craze. The surrounding grid bars of the film were carefully cut with a razor blade, and then the film was observed with a (JEOL Model 1200EX) transmission electron microscope operating at 120 keV.

Results and Discussion

(1) Unstrained Structure of an Interface. Figure 3a shows the typical structure of an unstrained interface

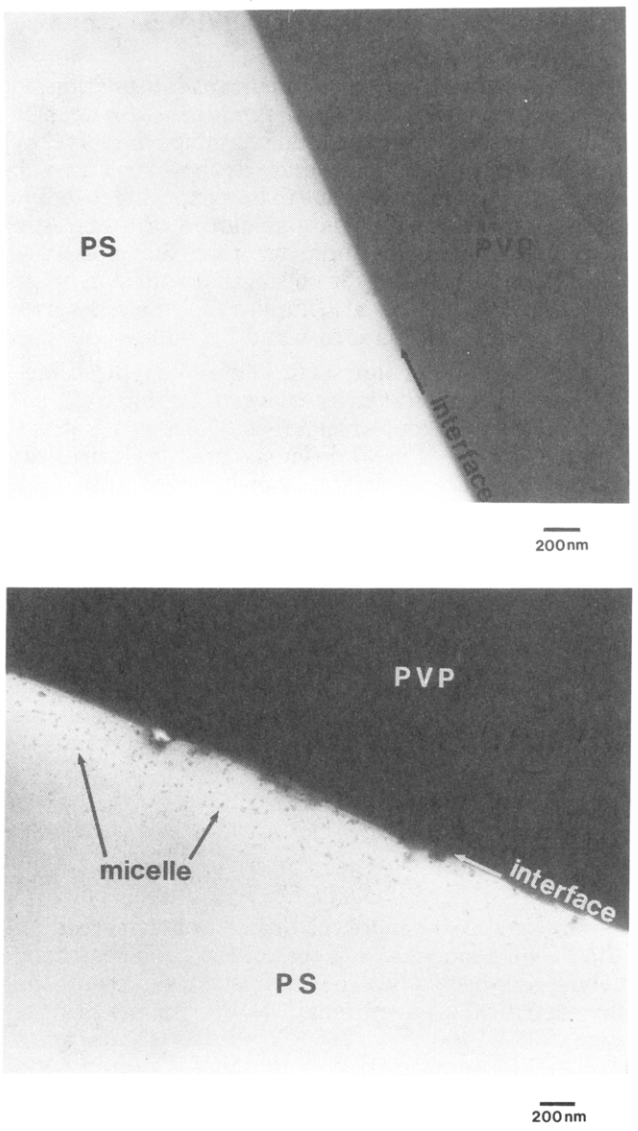

Figure 3. Unstrained structure of an interface reinforced with block copolymer A (960/950) with (a, top) $\Sigma = 0.0084$ and (b, bottom) 0.120 chains/nm^2 stained by exposure to iodine vapor. Note that, in a, no dark spots (the PVP core of block copolymer micelles) can be seen, while, in b, many dark spots can be seen in the PS.

at relatively low interfacial areal density of block copolymer A (960/950) with $\Sigma = 0.0084$ chains/nm^2, and Figure 3b shows this structure for a large areal density of A (Σ = 0.120 chains/nm^2). At low Σ's no micelles of block copolymer are observed in either the PS or the PVP phase (all the block copolymer spun onto the interface stays at the interface). At the high Σ's we observe micelles which appear as dark spots (PVP micelle cores) away from the interface in Figure 3b. It should be noted that the block copolymer chains forming these micelles, as well as any free block copolymer chains in the PS or PVP, cannot contribute to the interfacial adhesion because they form no junctions between the PS and PVP homopolymers.

One can estimate the maximum amount of free block copolymer chains in either PS or PVP using the empirical observation that PS–PVP block copolymers form micelles in preference to existing as free block copolymer at a block copolymer chemical potential of $\mu_c/k_bT \sim 5.5$.[12,14] The chemical potential is given by

$$\frac{\mu_c}{k_bT} \approx \ln \varphi_c + (1 - \varphi_c) - \frac{N_c}{P} + \chi[fN_c] \qquad (2)$$

Table II
Volume Fraction of the Block Copolymers Existing as Free Chains in Either PS or PVP

code	$N_{d\text{-}PS}/N_{PVP}$	φ_{cmc} in PS	φ_{cmc} in PVP
A	960/950	8.24×10^{-44}	2.74×10^{-44}
B	800/870	4.97×10^{-40}	3.65×10^{-37}
C	510/540	2.22×10^{-24}	6.03×10^{-23}
D	680/100	2.08×10^{-3}	4.08×10^{-31}

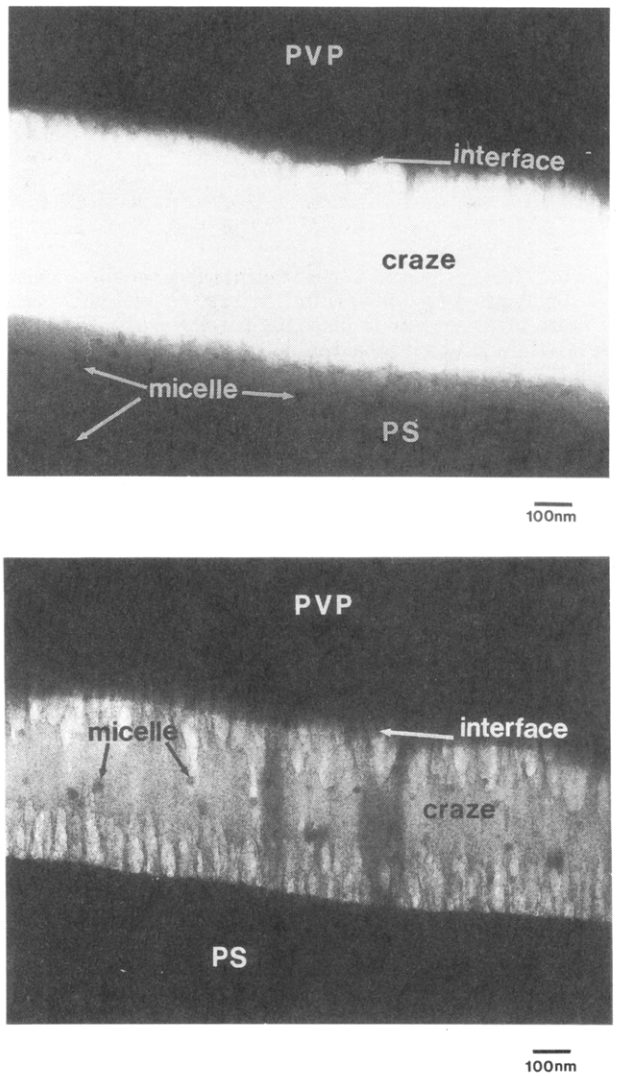

Figure 4. Craze propagation at the interface reinforced with block copolymer A (960/950) with $\Sigma = 0.120$ chains/nm^2. These two micrographs are reproduced from the same negative but with different exposure times: (a, top) short exposure to show details in the PS and (b, bottom) long exposure to show details in the craze. Note that the PVP core of the micelles can be seen in both the craze and the PS bulk, indicating that the craze grew in the PS.

for small block copolymer volume fractions, φ_c, where N_c and P are respectively the polymerization indices of the block copolymer and the homopolymer in which the block copolymer is dissolved and f is the fraction of unlike block (to the homopolymer) in the block copolymer. Using the experimentally measured value of $\chi = 0.11$,[12,14] we have estimated the critical micelle concentration, φ_{cmc}, from eq 2 and these estimates are shown in Table II; these estimatesare the upper limit for free block copolymer concentrations in both the PS and PVP phases. Except for block copolymer D (680/100) in PS, these concentrations are so small that they are completely negligible.

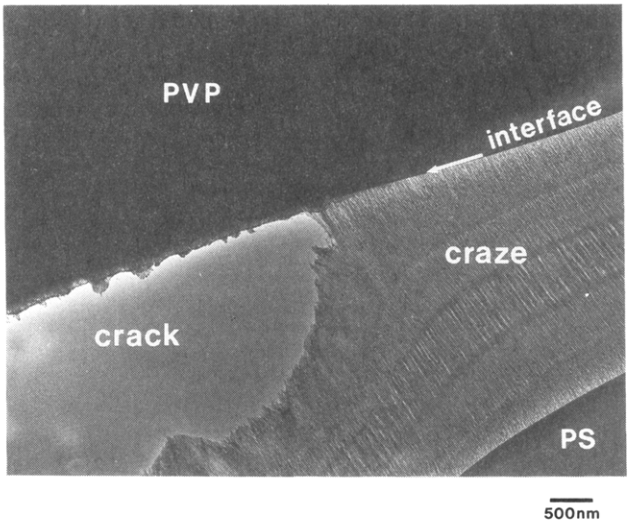

Figure 5. Crack propagation near the interface reinforced with block copolymer A (960/950) with $\Sigma = 0.120$ chains/nm^2. Note that craze breakdown took place exclusively at the PVP/PS-craze interface, indicating that the block copolymer is the weakest link in the material.

The micelles visible in Figure 3b, however, cannot be so easily ignored. However, we demonstrate using quantitative analysis of the TEM image plates that, in the worst case (Figure 3b), the amount of block copolymer in micelles away from the interface is less than 10% of the original areal density of block copolymer at the interface; i.e., at least 90% of the total block copolymer is still at the interface.[22] Hence, the areal density of block copolymer chains Σ measured with forward recoil spectrometry (FRES; depth resolution ~80 nm) by summing the amount found on both fracture surfaces is a reliable measure of the actual areal density of block copolymer chains at the interface.

(2) Craze Deformation at and near the Interface. Figure 4 shows a typical craze at an interface reinforced with block copolymer A (960/950) with $\Sigma = 0.120$ chains/nm^2 strained to 2%. The staining technique revealed that the craze had grown only in the PS side of the interface. If the craze had grown in the PVP side, one should find no dark spots of the PVP core of micelles in the craze. However, we have observed the dark spots, which can be seen only in the PS side of the unstrained interface (see Figure 3b), in the craze. We can therefore conclude that the craze grew only in the PS side. In the case of an interface between immiscible homopolymers reinforced with block copolymers, Brown[11] pointed out that a craze is generated only in the material with lower crazing stress. This observation thus indicates that the crazing stress of PS is lower than that of PVP, which is consistent with the experimental measurements of the crazing stresses at crack propagation rates typical of these experiments (~55 and ~75 MPa for PS and PVP, respectively[8]).

Using TEM, Creton et al.[7] have investigated the deformation and strength of interfaces between spherical domains of PVP and the surrounding PS matrix which were reinforced with a series of PS–PVP block copolymers in the blends of PS and PVP and observed that when $N_{PVP} > N_{e,PVP}$, the PVP phase was drawn into the PS craze within the active zone of the craze and fibrillated to become craze fibrils. In contrast, for the planar interfaces of the present study, the PVP phase was not drawn into the PS craze as shown in Figure 4. This comparison indicates that, for the spherical interface, a stress concentration developed at the PVP/craze interface, sufficient to cause elongation and fibrillation of PVP without causing fracture of the interface itself.

Figure 4 provides us other important information on the craze propagation trajectory. A mid-rib, which can be seen as a brighter line-shaped zone running parallel to the interface, is visible in the PS craze as shown in Figure 4: this mid-rib was broadened due to long exposure to iodine vapor. Since the mid-rib is a signature of a craze-tip trajectory,[20] this figure indicates that the craze was nucleated in the PS and grew in length parallel but offset from the interface. This also implies that the craze grew in width toward both interface and PS bulk.

(3) Crack Propagation. Figure 5 shows a typical crack which has propagated at an interface containing $\Sigma = 0.120$ chains/nm^2 of block copolymer A (960/950) after 5% strain. It is clear that craze breakdown occurred exclusively at the PVP/PS-craze interface, showing that the block copolymer is still the weakest point in this system.

According to Leibler,[4] for an A–B block copolymer at an A/B interface the block copolymer organizes itself as a "dry brush" so that the volume fraction of the homopolymer becomes zero within the brush (the volume fraction of the respective block equals 1) and 1 outside, resulting in little interpenetration between the block and its respective homopolymer, when the following conditions are met (the PS side of the interface is used as an example):

$$P_{PS}^{3/2} > N_{PS} \tag{3a}$$

and

$$a^2 P_{PS}^{1/2} \Sigma > 1 \tag{3b}$$

where P_{PS} and N_{PS} denote the degree of polymerization of the PS homopolymer and that of the PS block of the copolymer, respectively. The parameter a represents the Kuhn statistical segment length of PS. In the present system, $P_{PS} = 2400$, $N_{PS} = 960$, $\Sigma = 0.120$ (chains/nm^2), and $a = 0.67$ (nm) so that both these conditions are satisfied. Consequently, Leibler's model could predict that the craze breakdown occurred exclusively in this weakened zone.

Although the dry-brush model explains the locus of fracture of the interface, the model is oversimplified. For instance, the dry-brush model assumes the step-function type of concentration profile of both block and homopolymer near the interface,[4] implying that there would be no overlap, and hence no entanglements, between a block and its respective homopolymer. Since stress is transferred through entanglements from one strand to another, the dry-brush model will predict no stress transfer in the brush, resulting in no craze formation, or G_c would approach 2γ where γ is the (van der Waals) surface energy of PS. The interface would be no stronger than the bare PS/PVP interface, which is not the case at all.

For a more realistic and quantitative treatment, precise knowledge of entanglements between block copolymer and its respective homopolymer is necessary. Dai et al. have demonstrated experimentally that the self-consistent mean-field calculation (SCMF) developed by Shull et al.[13] can be used to predict both interfacial segregation[12,14] and the concentration profile[15] of PS–PVP block copolymers in the PS/PVP system. Using SCMF, Creton et al.[8] calculated the effective areal density of block copolymer, Σ_{eff}, which is the number of effectively entangled (load-bearing) block copolymer chains per unit area of the interface, as a function of Σ and showed that Σ_{eff} increased linearly with increasing Σ ($\Sigma_{eff} \sim \Sigma$) for small Σ and then saturated at a certain value depending on N_{PS}.

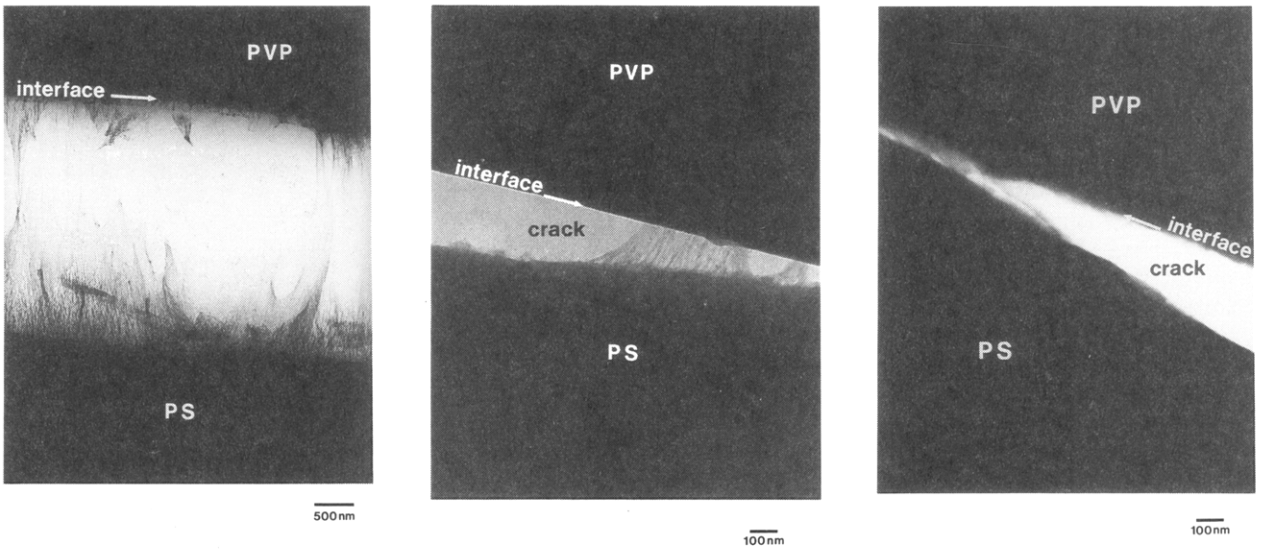

Figure 6. Crack propagation near the interface reinforced with block copolymer B (800/870) with (a, left) $\Sigma = 0.088$, (b, center) 0.015, and (c, right) 0.009 chains/nm^2. Note that, in a and b, a stable craze can be seen, while, in c, no stable craze can be seen at the interface. In a some part of the craze material and in b no craze material can be seen on the PVP side of the crack.

In the case of block copolymer A (960/950), the maximum value of Σ_{eff} is estimated to be approximately 0.06 chains/nm^2.[8] It should be noted in the case of crazing that a certain number of effective strands will be lost during the fibrillation process which takes place in the active zone of a craze so that the actual areal density of strands, Σ_{eff}, reinforcing the interface will be smaller than Σ_{eff}.[23] The probability, q, that a load-bearing strand survives during the fibrillation process is 0.6 for PS,[23] and from this estimate one can obtain $\Sigma'_{eff} = 0.036$ chains/nm^2.

On the other hand, Σ'_{eff} for the bulk PS homopolymer is given by[23]

$$\Sigma'_{eff} = \frac{1}{2}\nu'_e d \tag{4}$$

where ν'_e and d denote the effective strand density and the root-mean-square distance between entanglements, respectively. Inserting these parameters for PS, $\nu'_e = 1.85 \times 10^{25}$ m^{-3} and $d = 8.81 \times 10^{-9}$ m, into eq 4, one obtains $\Sigma'_{eff} = 0.082$ chains/nm^2. This value is much larger than that for the PS-block/PS-homopolymer interface, and therefore the fracture takes place exclusively in this block copolymer region of the interface and not in the bulk PS.

(4) Effect of Σ and N_{PVP}. We examined the effect of N_{PVP} on the interfacial fracture mechanisms as a function of the areal density of block copolymer chains at the interface, Σ, using block copolymers of B (800/870), C (510/540), and D (680/100).

(4.1) Long PVP Block ($N_{PVP} > N_{e,PVP}$). For the block copolymer B, it is clear, as shown in parts a and b of Figure 6, that craze formation occurred first in the PS followed by the breakdown of the craze at the PVP/craze interface when $\Sigma = 0.088$ and 0.015 chains/nm^2, respectively; the result is similar to those for block copolymer A. The craze breakdown mechanism of PS is believed to be dominated by chain scission when the testing temperature, T, is well below the T_g and the polymerization index, N, is much larger than N_e, while chain disentanglement (pull-out) becomes significant when T is close to the T_g or N is below N_e.[23,24] Since the polymerization indices of both blocks are much larger than the N_e of their respective homopolymers, the expected mechanism of craze breakdown is chain scission. Similar results were obtained for the block copolymer C (510/540).

At extremely low Σ, for instance when $\Sigma = 0.009$ chains/nm^2 of block copolymer B, we observed no stable craze at the interface (see Figure 6c), indicating that the transition in the fracture mechanism from crazing ($\Sigma > 0.015$ chains/nm^2) to noncrazing ($\Sigma = 0.009$ chains/nm^2) actually took place as pointed out by Hui et al. theoretically.[8,10]

Hui et al.[8,10] studied theoretically the fracture mechanisms of interfaces between immiscible polymers reinforced with block copolymers and have shown that when $N_{PVP} > N_{e,PVP}$, the transition in the fracture mechanism will take place at Σ_c from chain scission ($\Sigma < \Sigma_c$) to crazing ($\Sigma > \Sigma_c$). The critical value at the transition is given by eq 5.

$$\Sigma_c = \sigma_{PS;craze}/f_b \tag{5}$$

where f_b denotes the force required to break a single C–C bond. (Note that all main chains consist of C–C bonds.) Here we use $\sigma_{PS;craze}$ for crazing stress, because the crazing took place exclusively in the PS. Using eq 5, one can estimate f_b. It should be pointed out that Σ_{eff} (load-bearing chain density), instead of Σ, should be used to estimate Σ_c. However, at such small Σ, $\Sigma_{eff} = \Sigma$ is a good approximation as pointed out by Creton et al.,[8] one can thus use Σ for Σ_{eff}. Since when $\Sigma = 0.015$ chains/nm^2, a stable craze was observed at the interface as shown in Figure 6b, the transition is expected to take place in the range of $\Sigma = 0.009$–0.015 chains/nm^2. Inserting $\sigma_{PS;craze} = 55$ MPa and $\Sigma_c = 0.009$–0.015 chains/nm^2 into eq 5, one obtains $f_b = (3.7\text{–}6.1) \times 10^{-9}$ N/bond. This value is reasonable and consistent with previous works reported by Creton et al. (3.5×10^{-9} N/bond[8]), Brown (1.4×10^{-9} N/bond[11]), Odell et al. [$(2.6\text{–}13.4) \times 10^{-9}$ N/bond[25]], and Kausch (3.0×10^{-9} N/bond[26]).

Creton et al.[8] analyzed both PS and PVP sides of fracture surfaces of this system using FRES, Rutherford backscattering spectrometry (RBS), and X-ray photoelectron spectroscopy (XPS) to identify the location of the block copolymer chains and the locus of the chain fracture. In the system with block copolymer B (800/870), they found a clear transition in the distribution of d-PS block on the fracture surfaces and hence the locus of chain fracture. When $\Sigma < 0.03$ chains/nm^2, 90% of d-PS chains were observed on the PS side, when $\Sigma > 0.03$ chains/nm^2, 90% of the d-PS block was found on the PVP side. In addition, they observed a trace amount of PVP block copolymer chains on the PS side over the entire range of Σ investigated. They concluded that when $\Sigma < 0.03$ chains/nm^2,

chain scission occurred near the joint between the PS and the PVP blocks, while failure occurred between the d-PS block and PS homopolymer when $\Sigma > 0.03$ chains/nm^2. This transition took place at even lower Σ ($\sim$0.01 chains/nm^2) when the interface was reinforced with block copolymer C (510/540; smaller N_{PS}). Our TEM observation (see Figure 6a) showed that when $\Sigma = 0.088$ chains/nm^2 (above the transition), some part of the craze material was found on the PVP side (major part of the craze was found on the PS side), indicating that the craze breakdown took place inside the craze (in the PS homopolymer) but very close to the interface. Most of d-PS block was thus found on the PVP side of the interface. In contrast, when $\Sigma = 0.015$ chains/nm^2 (below the transition), the PVP side of the fracture interface was smooth, and hence almost no part of the craze material remained on the PVP side, indicating that the craze breakdown took place at the interface and hence almost all the d-PS block was found on the PS side of the fracture surface. These observations are consistent with those of Creton et al.[8] reported above.

(4.2) Short PVP Block ($N_{PVP} < N_{e,PVP}$). For block copolymer D with $\Sigma = 0.103$ chains/nm^2, we have observed the same fracture processes as observed in B and C as shown in Figure 7a, i.e. a craze developed first in the PS directly adjacent to the interface, and craze breakdown occurred exclusively at the PVP/PS-craze interface. Creton et al.[8] analyzed the halves of the fracture surfaces of this system and found that both the d-PS and the PVP blocks remained on the PS side of the fractured surface, which led them to conclude that block copolymer chains were pulled out from the PVP bulk, corresponding to one-sided chain pullout. Xu et al.[10] developed a theoretical model where one-sided chain pullout is the main energy-consuming mechanism for the fracture toughness, G_c, of interfaces between immiscible homopolymers reinforced with block copolymers. The model predicts G_c to be proportional to Σ, which was in qualitative agreement with fracture toughness experiments. The model is for pure one-sided pullout where the opposite block remains firmly anchored, and, in this case, crazing would not be expected. However, as Xu et al. pointed out, for block copolymer D (680/100) the values of G_c experimentally obtained ($\sim$6.5 J/m^2) were 5 times larger than those predicted by the pure one-sided chain pullout model ($\sim$1.3 J/m^2; for maximum value),[10] implying that another fracture mechanism should be considered. In light of the present observations (see Figure 7a), this large discrepancy in G_c is attributed to the existence of a craze on the PS side of the interface. Since the polymerization index of the PVP block (100) is much smaller than $N_{e,PVP}$, the expected craze breakdown mechanism is chain disentanglement. Consequently, the fracture mechanism of the interface reinforced with block copolymer D (680/100) is crazing in the PS followed by the craze breakdown by pullout of the PVP block from the bulk PVP. At low Σ (=0.0050 chains/nm^2), however, stable crazes were not observed as shown in Figure 7b, and here perhaps the mechanism of pure one-sided chain pullout proposed by Xu et al.[10] actually operates. The PVP side of the fracture interface was smooth, and no craze material remained on the PVP side for all Σ examined, supporting the surface analysis results of Creton et al.[8] where no d-PS block was found on the PVP side.

From these observations, the fracture mechanism map[8,10] for interfaces between immiscible polymers reinforced with block copolymers actually worked for both $N_{PVP} > N_{e,PVP}$ and $N_{PVP} < N_{e,PVP}$.

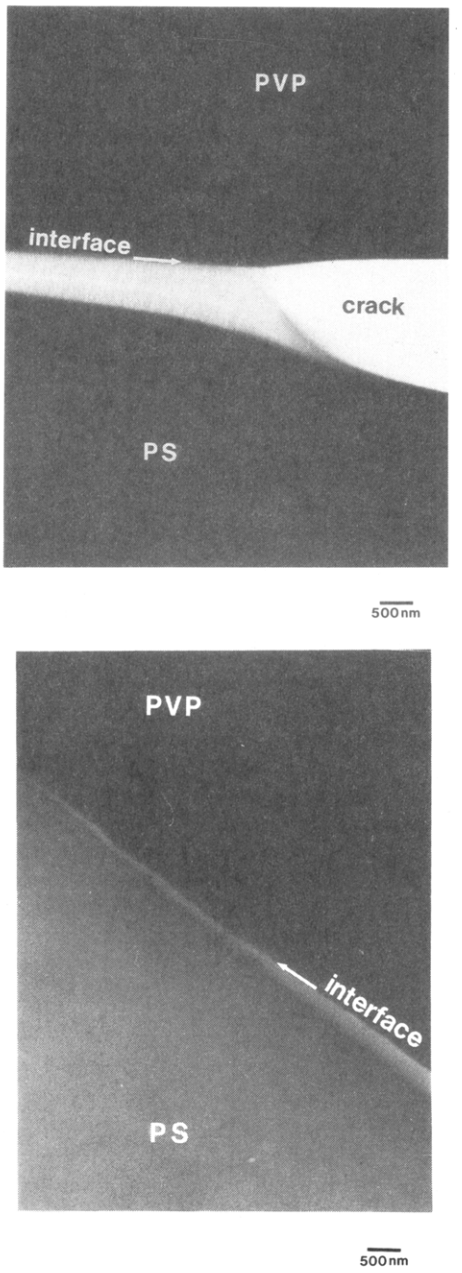

Figure 7. Crack propagation near the interface reinforced with block copolymer D (680/100) with (a, top) $\Sigma = 0.103$ and (b, bottom) 0.0050 chains/nm^2. Note that, in a, a stable craze can be seen, while, in b, there is no stable craze at the interface.

(5) Contribution of Crazing to Fracture Toughness. For the interfaces reinforced with both the long PVP block (A–C) and the short PVP block (D) block copolymers with large Σ's, crazing preceded fracture of the interface for high areal densities of block copolymer. It is worthwhile to estimate the contribution of crazing to the interfacial fracture energy. Since no shear deformation was observed, one can expect that crazing is the dominant energy dissipation mechanism in the interfacial fracture. According to Brown,[11] one can calculate the G_c due to crazing from the craze width given by

$$G_c = \sigma_{PS:craze} h(1 - 1/\lambda) \quad (6)$$

where h is the craze width at the crack tip and λ is the extension ratio of craze fibrils. Obtaining h from TEM micrographs, one can calculate G_c using $\sigma_{PS;craze} = 55$ (MPa) and $\lambda = 4$, the latter having been previously established by TEM measurements of craze fibril volume fractions for PS.[20,23] Creton et al.[8] measured the fracture toughness

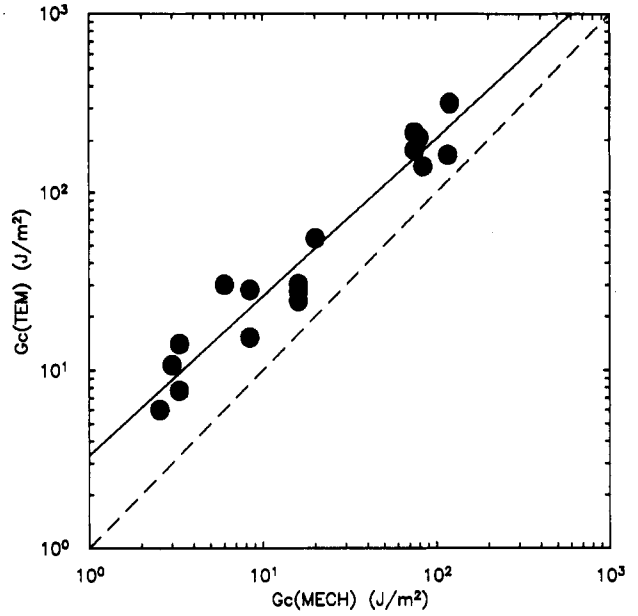

Figure 8. Relationship between G_c(TEM) vs G_c(MECH). Note that G_c(TEM) is comparable to G_c(MECH) over the entire range of G_c examined and that G_c(TEM) ~ $2G_c$(MECH).

of these systems using an asymmetric double cantilever beam geometry. We can then compare the G_c measured from the TEM experiments, G_c(TEM), with that measured from the mechanical tests, G_c(MECH).

Since craze strength and crazing stress are both sensitive particularly to strain rate, or more precisely craze interface velocity, v (which is proportional to but less than the crack velocity), it is crucial to check the value of v for the mechanical tests, the TEM experiments, and the crazing stress measurements. The velocity v for the TEM study was in the range of v = 50–200 nm/s, and that for the mechanical tests and crazing stress measurements were respectively v = 40–170 and ~60 nm/s,[8] ensuring that, as far as the craze interface velocity, these three experimental conditions were close and the results can be compared directly. Clearly, however, since the crack and craze are not actually propagating when observed by TEM, we are making the tacit assumption that their structure is maintained after the strain rate of the copper grid is equal to zero.

From Figure 8, where G_c(MECH) is plotted vs G_c(TEM), it is clear that G_c(TEM) is comparable to G_c(MECH) over the entire range of G_c examined, indicating that when Σ is large, crazing is the dominant energy dissipation mechanism in these systems and governs the fracture toughness of the interfaces. The values of G_c(TEM) are, however, about twice as large as those of G_c(MECH). This discrepancy will be discussed in more detail in the next section.

(6) Discrepancy between G_c(TEM) and G_c(MECH). It is well-known that a crack propagating at an interface between two elastically dissimilar materials will be characterized by a mode II stress intensity factor K_{II} (in-plane sliding) as well as the mode I stress intensity factor K_I (opening mode)[27] even under loading geometries for which K_{II} would be zero for a homogeneous material. This tendency toward mixed mode propagation was characterized by the mixity Ψ which is given by

$$\tan \Psi = K_{II}/K_I \quad (7)$$

Cracks and the crazes which precede them, however, tend to propagate in a direction which minimizes K_{II} and Ψ. This tendency is pronounced for polymer/polymer interfaces especially when one polymer has a lower Young's modulus and a lower crazing stress than the other.[28]

In the case of PS/PVP interfaces in symmetrically loaded specimens, a Ψ driving the craze and crack toward the PS phase is expected, since Young's modulus of PVP is higher than that of PS and Poisson's ratios of the two materials are very close. We define such a mixity Ψ as positive. The craze tip would tend to propagate into the PS, resulting in a larger G_c compared with that of the interface itself even if the craze cracks along the interface. In order to obtain the true value corresponding to a slightly negative Ψ, Creton et al.[8] measured G_c using an asymmetric double cantilever beam geometry which compensated for the difference in the modulus. They hypothesized that, with this geometry, the craze tip was pushed to and remained on the interface without deviating into the PVP, because PVP is more craze resistant than PS. The interfacial craze can therefore grow in width only toward the bulk PS direction. In contrast, the geometry in the present TEM study is symmetric, yielding a positive mixity Ψ, and hence the craze can grow in width toward both the interface and PS bulk.

It stands to reason that under these conditions, where the craze can widen in both directions before it reaches the interface, the final craze width at fracture and thus G_c will be larger than when the craze tip is held at the interface and the craze can only widen asymmetrically. The fact that we observe that G_c(TEM) ~ $2G_c$(MECH) is therefore not surprising. How much the craze tip is offset from the interface is obviously important, but a more detailed model which predicts the magnitude of this offset quantitatively is not available at present.

In order to examine the effect of mixity Ψ on a craze-tip trajectory, a negative Ψ was introduced to the interfacial stress field of the TEM specimen by tilting the interface by 9° from the plane of the maximum principal stress and following the same procedure described before. In this experiment, the exposure time to iodine vapor was shorter than usual (2 h, rather than the usual 6–12 h) so that the craze fibril structure, particularly mid-rib position, is expected to be close to the original (without exposure to iodine) one. Under this exposure condition, we observed a mid-rib in a craze formed in PS homopolymer, ensuring that a mid-rib can be observed in the interfacial craze, if it exists.

As shown in Figure 9a, no mid-rib can be seen in the craze of the tilted sample, indicating that the craze tip stayed on the interface. In addition, the shape of the craze tip, as shown in Figure 9b, is asymmetric, flat on the PVP side and curved on the PS side. These observations indicate that the craze tip propagated on the interface and that the craze grew in width only toward the PS bulk, consistent with the above discussion.

This difference in the craze-tip trajectory, however, should not change the fracture mechanisms of the interfaces as long as only a small negative Ψ is introduced at the craze-tip stress field; it would change only the absolute values of G_c. If a large negative Ψ was introduced, on the other hand, the craze tip would be driven into the PVP, resulting in a larger G_c, as much as when a positive value of Ψ was introduced. The result will be a minimum in G_c with a small negative Ψ; such a minimum was indeed observed by Creton et al.[8]

Conclusions

1. A method has been developed to allow TEM observation of the fracture mechanisms at PS/PVP interfaces reinforced with PS–PVP block copolymers, by microtoming thick (0.5–1.0-μm) slices in a direction perpendicular to the interfacial plane and straining these

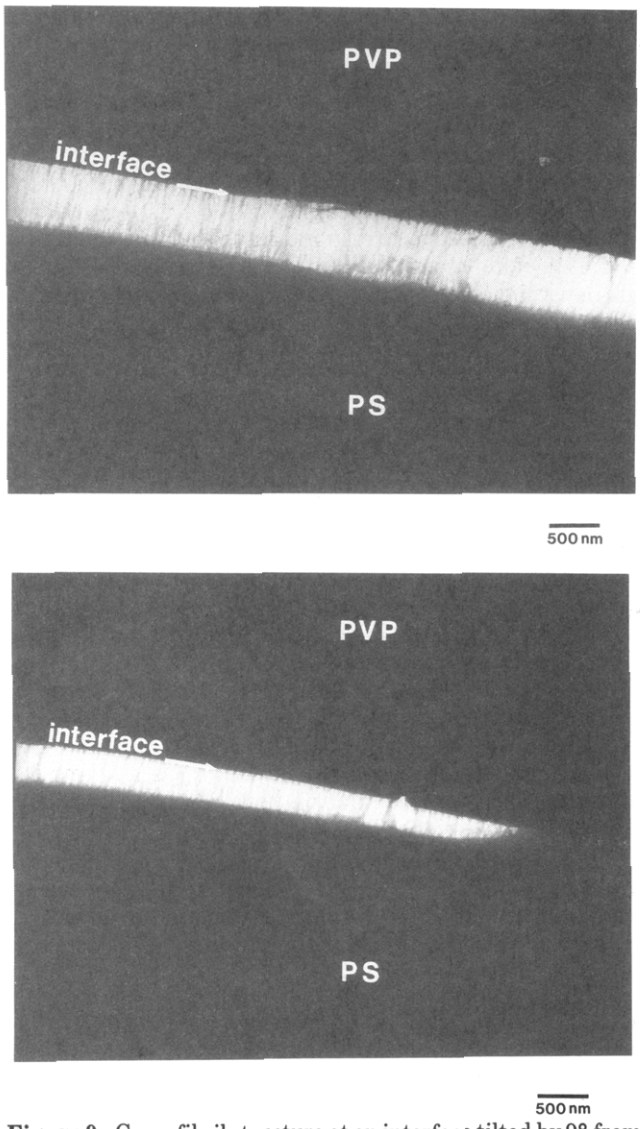

Figure 9. Craze fibril structure at an interface tilted by 9° from the plane of the maximum principal stress: (a, top) middle part of the craze and (b, bottom) near the craze tip. The interface was reinforced with block copolymer A (960/950) and $\Sigma = 0.120$ chains/nm^2. Note that, in a, no mid-rib can be seen in the craze and that, in b, the shape of the craze tip is asymmetric, flat against the interface on the PVP side and curved on the PS side.

slices mounted on a copper grid. The technique would seem to be generally applicable to a wide variety of polymer interfaces.

2. At high areal density, Σ, of block copolymer chains, micelles of the block copolymer were observed in the PS near the interface, but these constitute only a minor part of the block copolymer chains at the interface.

3. At large Σ, the fracture mechanism is crazing in the PS side of the interface followed by craze breakdown, which occurred exclusively at the PVP/craze interface, to form a crack, indicating that the block copolymer is still the weakest link in this system.

4. At small Σ, on the other hand, noncrazing fracture was observed. When $N_{PVP} > N_{e,PVP}$, fracture took place by chain scission, while when $N_{PVP} < N_{e,PVP}$, the fracture mechanism was one-sided chain pullout of the PVP block from the PVP bulk.

5. In the case of crazing, the values of G_c calculated from TEM micrographs are comparable (G_c(TEM) $\sim 2G_c$(MECH)) to those obtained from mechanical tests over a wide range of G_c, indicating that crazing is the dominant energy dissipation mechanism in this system, and governs the fracture toughness of all but the weakest interfaces.

Acknowledgment. We gratefully acknowledge that this work benefited from use of the facilities of the Cornell Materials Science Center which is funded by the National Science Foundation. We also appreciate the important contributions of K. H. Dai and Dr. K. R. Shull in the synthesis of the block copolymers and Professor C. Y. Hui and Dr. J. W. Smith for stimulating discussions. J.W. is supported by a grant from Showa Denko K.K., Japan.

References and Notes

(1) Fayt, R.; Jerome, R.; Teyssie, Ph. *J. Polym. Sci., Polym. Phys. Ed.* **1989**, *27*, 775.
(2) Fayt, R.; Teyssie, Ph. *Polym. Eng. Sci.* **1989**, *29*, 538.
(3) Anastasiadis, S. H.; Gancarz, I.; Koberstein, J. T. *Macromolecules* **1989**, *22*, 1449.
(4) Leibler, L. *Makromol. Chem., Makromol. Symp.* **1988**, *16*, 1.
(5) Brown, H. R. *Macromolecules* **1989**, *22*, 2859.
(6) Brown, H. R.; Deline, V. R.; Green, P. F. *Nature* **1989**, *341*, 221.
(7) Creton, C.; Kramer, E. J.; Hadziioannou, G. *Macromolecules* **1991**, *24*, 1846.
(8) Creton, C. Ph.D. Thesis, Cornell University, Ithaca, NY, 1992. Creton, C. F.; Kramer, E. J.; Hui, C. Y.; Brown, H. R. *Macromolecules* **1992**, *25*, 3075.
(9) Hui, C. Y.; Ruina, A.; Creton, C.; Kramer, E. J. *Macromolecules*, in press.
(10) Xu, D. B.; Hui, C. Y.; Kramer, E. J.; Creton, C. *Mech. Mater.* **1991**, *11*, 257.
(11) Brown, H. R. *Macromolecules* **1991**, *24*, 2752.
(12) Shull, K. R.; Kramer, E. J.; Hadziioannou, G.; Tang, W. *Macromolecules* **1990**, *23*, 4780.
(13) Shull, K. R.; Kramer, E. J. *Macromolecules* **1990**, *23*, 4769.
(14) Dai, K. H.; Kramer, E. J.; Shull, K. R. *Macromolecules* **1992**, *25*, 220.
(15) Dai, K. H.; et al., to be published.
(16) Feldman, L. C.; Mayer, J. W. In *Fundamentals of Surface and Thin Film Analysis*; North-Holland: Amsterdam, The Netherlands, 1986.
(17) Mills, P. J.; Green, P. F.; Palmstrom, C. J.; Mayer, J. W.; Kramer, E. J. *J. Appl. Phys. Lett.* **1984**, *45*, 958.
(18) Shull, K. R. Ph.D. Thesis, Cornell University, Ithaca, NY, 1990.
(19) Beahan, P.; Bevis, M.; Hull, D. *Philos. Magn.* **1971**, *24*, 1267.
(20) Lauterwasser, B. D.; Kramer, E. J. *Philos. Magn.* **1979**, *A39*, 469.
(21) Aronson, S.; Wilensky, S. B. *J. Polym. Sci., Polym. Chem. Ed.* **1988**, *26*, 1259.
(22) Washiyama, J.; et al., to be published.
(23) Kramer, E. J. *Adv. Polym. Sci.* **1983**, *52/53*, 1.
(24) Kramer, E. J.; Berger, L. L. *Adv. Polym. Sci.* **1990**, *91/92*, 1.
(25) Odell, J. A.; Keller, A. *J. Polym. Sci., Polym. Phys. Ed.* **1986**, *24*, 1889.
(26) Kausch, H. H. In *Polymer Fracture*, 2nd ed.; Springer-Verlag: Berlin, 1987.
(27) Rice, J. R. *J. Appl. Mech.* **1988**, *55*, 98.
(28) Brown, H. R. *J. Mater. Sci.* **1990**, *25*, 2791.

Registry No. PS, 9003-53-6; PVP, 25014-15-7; (PS)(PVP) (block copolymer), 108614-86-4.